Reconstitution of immune cell populations in multiple sclerosis patients after autologous stem cell transplantation

Fredrick G. Karnell[1], Dongxia Lin[2], Samantha Motley[3], Thomas Duhen[3], Noha Lim[1], Daniel J. Campbell[3], Laurence A. Turka[1,4], Holden T. Maecker[2], and Kristina M. Harris[1]

[1] Immune Tolerance Network, Bethesda, MD, USA.

[2] Institute for Immunity, Transplantation and Infection, Stanford University, Stanford, USA.

[3] Benaroya Research Institute, Seattle, WA 98101; and Department of Immunology, University of Washington School of Medicine, Seattle, WA 98195

[4]Massachusetts General Hospital, Center for Transplantation Sciences, Boston, Massachusetts, USA

Correspondence: Kristina M. Harris, Immune Tolerance Network, 7500 Old Georgetown Road, Suite 800, Bethesda, MD, USA 20814
kharris@immunetolerance.org

Keywords: Immune cell reconstitution, CyTOF mass cytometry, flow cytometry, T cells, multiple sclerosis

ABSTRACT

Multiple sclerosis is an inflammatory T-cell-mediated autoimmune disease. In a phase II clinical trial, high-dose immunosuppressive therapy combined with autologous $CD34^+$ hematopoietic stem cell transplant resulted in 69.2% of subjects remaining disease-free without evidence of relapse, loss of neurological function or new MRI lesions through year 5 post-treatment. A combination of CyTOF mass cytometry and multi-parameter flow cytometry was used to explore the reconstitution kinetics of immune cell subsets in the periphery post HSCT and the impact of treatment on the phenotype of circulating T cells in this study population. Repopulation of immune cell subsets progressed similarly for all patients studied 2 years post therapy, regardless of clinical outcome. At month 2, monocytes and NK cells were proportionally more abundant, while CD4 T cells and B cells were reduced, relative to baseline. In contrast to the changes observed at earlier time points in the T cell compartment, B cells were proportionally more abundant and expansion in the proportion of naïve B cells was observed 1 and 2 years post therapy. Within the T cell compartment, the proportion of effector memory and late effector subsets of CD4 and CD8 T cells was increased, together with transient increases in proportions of CD45RA- Tregs, and Th1 cells, and a decrease in Th17.1 cells. While none of the treatment effects studied correlated with clinical outcome, patients that remained healthy throughout the 5-year study had significantly higher absolute numbers of memory CD4 and CD8 T cells in the periphery prior to stem cell transplantation.

INTRODUCTION

Multiple sclerosis (MS) is a chronic autoimmune disease of the central nervous system (CNS) in which infiltration of autoreactive immune cells into the CNS and release of inflammatory cytokines is thought to promote neuronal demyelination and damage. The role of CD4 T cells has long been considered central to MS pathophysiology (*1, 2*), however, increasing evidence suggests additional immune cell types, including B cells and NK cells, play a role in this complex disorder (*3-6*). Alterations in the distribution and function of circulating T and B cell populations have been shown to correlate with disease activity and reflect those observed in the CNS of patients with MS, identifying potential immunological biomarkers for monitoring diseasing activity and response to treatment (*6*).

One intervention strategy that has shown promise as a durable therapy for MS, is a single course of high-dose immunosuppressive therapy (HDIT), followed by autologous hematopoietic cell transplant (HSCT) (*7-10*). In the Hematopoietic Cell Transplantation for Relapsing-Remitting Multiple Sclerosis (HALT-MS) phase II trial of HDIT/HSCT, overall event-free survival 5 years post therapy was 69.2% (*11*). The mechanistic rationale of this therapy is to first remove pathogenic autoreactive cells thought to perpetuate disease, and replace them with a de novo repertoire of immune cells that hopefully promote immune tolerance to disease-specific antigens. In this study, the analytical power of mass cytometry (CyTOF), together with multi-parameter flow cytometry were used to expand upon our initial findings (*12, 13*) and define the repopulation kinetics, composition, activation and cytokine profiles of discrete T cell subsets in the peripheral blood of MS patients before and after HDIT/HSCT treatment in the HALT-MS trial. This comprehensive analysis of peripheral blood leukocytes allowed us to examine the dynamics of

leukocyte repopulation in lymphopenic MS patients. While we did not see a correlation between treatment success or other patient parameters and cellular re-population, we did find that patients who remained healthy throughout the 5-year study had significantly higher absolute numbers of memory CD4 and CD8 T cells in the periphery prior to HDIT/HSCT treatment.

METHODS AND MATERIALS

PBMC cryopreservation and thawing. PBMCs were isolated by Ficoll separation and cryopreserved. They were stored and shipped in vapor phase liquid nitrogen until thawing which was carried out as described (*14*). After washing and counting, cells were re-suspended at 10^7 cells/ml in complete medium, and plated at 200 μl per well in a 96-well microtiter plate.

CyTOF staining and acquisition. Replicate wells of PBMC from each patient time point were either stimulated with 10 ng/ml PMA + 1 μg/ml ionomycin, or left unstimulated, for 4 h at 37°C, in the presence of 5 μg/ml brefeldin A and 5 μg/ml monensin. Cells were then stained (*15*) using the cocktail shown in Table 1. After intracellular staining and washing, cells were kept at 4°C and analyzed by CyTOF within 24 hours. On the day of acquisition, cells were treated with DNA intercalator, then washed with CyFACS buffer and ultrapure deionized water (*15*). Approximately 300,000 total events per sample were collected on a CyTOF™ mass cytometer (Fluidigm, South San Francisco, CA), using Dd mode. FCS files were exported and analyzed using FlowJo (TreeStar, Eugene, OR), with gating as shown in Supplementary Figure 1.

SPADE analysis. Equal numbers of live singlets from each FCS file for a given time point were concatenated to form a single FCS file. The resulting four concatenated files were analyzed in CytoSPADE (*16*), with a target node number of 400, and down sampling of 10%. Dimensions used for clustering are shown in bold in Table 1.

Table 1. CyTOF panel

Metal label	Specificity	Antibody Clone	Source
Qdot	**CD3**	S4.1	Invitrogen
115In	MaleimideDOTA		Macrocyclics
139La	**CD49d**	9F10	Biolegend
141Pr	**CD45RO**	UCHL1	Biolegend
142Nd	**CD19**	HIB19	DVS
143Nd	**CD57**	HCD57	Biolegend
144Nd	CD69	FN50	AbD Serotec
145Nd	**CD4**	RPA-T4	DVS
146Nd	**CD8**	HIT8a	Biolegend
147Sm	**CD20**	2H7	DVS
148Nd	MIP1β	D21-1351	BD Special
149Sm	**CD85j**	292319	R+D Systems
150Nd	**CD45RA**	HI100	Biolegend

151Eu	**CD38**	HB-7	BD Special
152Sm	TNFα	Mab	DVS
153Eu	Granzyme B	GB11	AbCam
154Sm	CD107a	H4A3	BD
155Gd	GMCSF	BVD2-21C11	Biolegend
156Gd	**CD94**	HP-3D9	BD
157Gd	IL-2	MQ1-17h12	eBiosci.
158Gd	IFNγ	4S.B3	eBiosci.
159Tb	**HLA-DR**	G46-6	BD
160Gd	**CD14**	M5E2	DVS
161Dy	**CD43**	84-3C1	eBiosci.
162Dy	Biotin-IL-10	JES3-12G8	Biolegend
163Dy	CD154	24-31	Biolegend
164Dy	IL-17A	N49-653	DVS
165Ho	**CD127**	A019D5	Biolegend
166Er	**CD33**	P67.6	Santa Cruz Biotechnology
167Er	**CD27**	L128	DVS
168Er	**CD28**	L293	BD
169Tm	**CCR7**	150503	R&D Systems
170Er	**PD1**	EH12.1	BD
171Yb	**TCRgd**	B1	Biolegend
172Yb	**IgD**	IA6-2	Biolegend
173Yb	Perforin	B-D48	AbCam

174Yb	**CD16**	3G8	Biolegend
175Lu	**CD56**	NCAM16.2	BD
176Yb	**CD25**	M-A251	BD

Graphing and statistics. Gated percentages were converted to absolute cell counts by reference to complete blood counts. The absolute counts were plotted using GraphPad Prism. Group differences were assessed using multiple t test, with correction for multiple comparisons by the Holm-Sidak method.

Flow cytometry staining and rhodamine efflux

Frozen PBMCs (10-15 million cells) were thawed and rested overnight at 37°C in a 6-well tissue culture plate (Greiner). The following morning the cells were harvested and washed with ice cold efflux buffer (RPMI 1640 + glutamine + hepes + 1% bovine calf serum) then spun down at 1500 RPM for 5 minutes at 4°C. The cells were resuspended in 1.5 ml of cold efflux buffer + 10 µg/ml rhodamine-123 (Sigma) and left on ice for 30 minutes. Cells were then washed twice with cold efflux buffer and spun down at 1500 RPM for 5 minutes at 4° before being resuspended in 1.5 ml of 37°C efflux buffer and placed in a 37°C water bath for 1.5 hours. Surface staining for CD3 (clone UCHT1, Biolegend), CD4 (clone OKT4, Biolegend), CD8 (clone RPA-T8, Biolegend), CD45RA (clone HI100, Biolegend), CD127 (clone A019D5, Biolegend), CD25 (clone BC96, Biolegend), CD161 (clone HP-3G10, Biolegend), CCR4 (clone L291H4, Biolegend), CCR6 (clone R6H1, eBioscience) and CXCR3 (clone 1C6, BD) was subsequently performed in FACS buffer (PBS w/o Ca^{2+} + Mg^{2+} supplemented with 2% BCS and 1 mM EDTA) for 30 minutes

on ice. Flow cytometry was performed on a FACS Aria II (BD), and analysis performed using FlowJo (Tree Star).

Patient information

Clinical data from the HALT-MS participants is outlined in table 2 and has previously been reported (ref. 11) and is available on ITNTrialShare (https://www.itntrialshare.org/study/Studies/ITN033AI5YR/Study%20Data/dataset.view?datasetId=502).

Table 2. Patient Data

Patient number	Endpoint	Age at Mobilization	Gender	Race	Baseline EDSS Score	Months in Follow-up
HALT_326456	No relapse	26	Female	White	4.50	61.4
HALT_990611	Relapse	28	Female	White	5.00	61.2
HALT_858871	Relapse	46	Female	White	4.50	31.7
HALT_566004	No relapse	38	Female	White	3.00	72.4
HALT_787656	Relapse	27	Male	White	4.50	48.3
HALT_544537	No relapse	28	Male	Multi-Racial	4.50	70.3
HALT_990883	No relapse	34	Male	White	5.00	71.2
HALT_831638	Relapse	27	Female	White	4.50	64.7
HALT_295836	No relapse	34	Male	White	4.50	41.3
HALT_957030	Relapse	33	Female	White	4.00	46.4
HALT_389670	Relapse	26	Female	White	5.50	68.1
HALT_324300	No relapse	42	Male	White	4.00	60.9
HALT_613743	No relapse	41	Female	White	4.00	66.8
HALT_284319	No relapse	52	Female	White	4.00	62.2
HALT_416568	No relapse	43	Female	White	3.50	65.9
HALT_677447	No relapse	39	Female	White	4.00	63.4
HALT_268578	No relapse	31	Female	White	5.00	61.1
HALT_201862	No relapse	37	Female	White	4.00	62.9
HALT_452644	No relapse	47	Female	White	4.00	56.8
HALT_454298	No relapse	40	Male	White	4.00	12.0
HALT_663301	Relapse	49	Female	White	5.50	53.9

HALT_302299	No relapse	37	Female	White	4.00	62.9
HALT_169679	No relapse	31	Male	White	5.00	62.5

RESULTS

Time course of immune cell reconstitution post-stem cell transplant.

Immunophenotyping by CyTOF mass cytometry was performed on cryopreserved PBMC from 23 HALT-MS participants treated with HDIT/HSCT before and after intervention at month 2, year 1 and year 2. The CyTOF panel comprised a combination of 29 cell surface and 9 intracellular markers (Table 1), providing a powerful immunological tool for monitoring the frequency and activation state of discrete leukocyte populations. SPADE analysis was employed to group related cell clusters into major leukocyte populations (CD4 T cells, CD8 T cells, B cells, NK cells, and monocytes), and to determine the proportions of specific cell subsets within these parent populations. SPADE trees were generated to visualize the overall kinetics of immune cell reconstitution in the peripheral blood of all 23 participants following HDIT/HSCT. Absolute counts were calculated from SPADE analysis together with total lymphocyte counts obtained from patient complete blood counts (CBC), and used to generate pie charts for evaluating the relative composition of specific cell subsets within each major leukocyte population (Figure 1). A transient increase in the proportion of total monocytes and NK cells was observed 2 months post-transplant that returned to baseline at year 1 (Figure 1, SPADE trees). This is in contrast, and likely related to the reduced numbers of circulating CD4 T cell and B cell populations previously reported at this early time point post-HSCT (*12, 13*). Within the CD4 and CD8 T cell compartments in peripheral blood at month 2, we observed a temporary redistribution of subsets with increased proportions of effector memory (CD45RA-CCR7-) and late effector

(CD45RA+CCR7-) subtypes that returned to baseline at years 1 and 2 (Figure 1 pie charts). Total B cells were modestly reduced at month 2, but increased from baseline at years 1 and 2 post-transplant (Figure 1 SPADE, trees). Within the circulating B cell population at years 1 and 2 post-transplant, proportions of naïve B cells expanded compared to baseline (Figure 1, pie charts). All major immune cell types, except for CD4 T cells, were fully recovered 2 years post-transplant.

Impact of HDIT/HSCT on discrete subsets of CD4 T cells in peripheral blood

Relapsing-remitting MS is considered to be mediated by autoreactive Th1/Th17.1 effector cells (*17-20*), and alterations in regulatory function and homeostasis of naïve and memory-like $CD4^{+}Foxp3^{+}/CD25^{+}CD127^{+}$ Tregs (*21-29*). To evaluate the impact of HDIT/HSCT treatment on these subsets, multi-parameter flow cytometric analysis was performed on cryopreserved PBMC from the 17 of the 23 HALT-MS participants for which we had samples. Frequencies of CD4 Tregs ($CD25^{+}CD127^{lo/-}$) and effector T helper cell lineage subsets were assessed before and after intervention at month 6 and year 2.

At month 6 and year 2 post-transplant, the percentage of total CD4 Tregs in peripheral blood was not significantly different from baseline (Figure 2A, graph). However, the ratio of $CD45RA^{-}$:$CD45RA^{+}$ subsets within circulating Tregs was significantly different from baseline at month 6 with the majority displaying a memory (CD45RA-) phenotype that returned to baseline distribution at year 2 (Figure 2A, pie charts). Although the percentage of memory CD4 non-Tregs (CD45RA-CD25-CD127+) appeared to increase in peripheral blood at month 6 compared to baseline and year 2, this was not statistically significant (data not shown).

We next examined the composition of effector T helper cell lineage subsets using combinations of chemokine receptors on the surface of memory CD4 non-Tregs (*30*). Each of these populations was measured relative to total CD4 cells. The proportion of CXCR3+CCR6-Th1 effector memory cells increased at month 6 and began to decrease at year 2, but did not fully return to baseline values. The proportion of CXCR3-CCR6+ Th17 effector memory cells did not change across all observed time points (Figure 2B). Although the proportion of Th17.1 CXCR3+CCR6+ Th17.1 effector memory cells relative to total CD4 cells was low, this cell subset was significantly lower than baseline at both month 6 and year 2 (Figure 2B).

Th17.1 cells expressing MDR1 have been shown to be potent co-producers of IFNg, IL-17, GM-CSF, lack IL-10 and are considered to be highly pro-inflammatory and are believed to be a primary contributor to pathogenesis in multiple sclerosis (*31*). A rhodamine efflux assay was used to measure MDR1 activity for Th1, Th17, and Th17.1 effector T cells (*31*). While MDR1 activity was decreased on all effector T cells following transplant especially at 6 months, the Th17.1 cells with was particularly susceptible to treatment and MDR1 activity did not rebound even out to year 2 (Figure 2C). It should also be noted that no differences were seen between patients that did or did not maintain event-free survival through year 5.

Impact of HDIT/HSCT on T cell Cytokine and Activation Profiles

To further analyze cell phenotype, we used CyTOF mass cytometry to track changes in intracellular cytokine production and activation markers on the surface of discrete T cell populations before and after HSCT treatment at month 2 and years 1 and 2. SPADE analysis (14) was used to construct trees by clustering related populations from all 23 subjects at each

time point as described for Figure 1. Given the complexity of the data and small number of patients, statistical analyses of the changes in all markers in all cell subsets at each time point was not performed. Upon visual examination, however, changes in the overall expression of PD-1 and the number the number of IFNg expressing cells were striking. We therefore examined cell subsets using SPADE trees colored by IFNg (Figure 3A) and PD-1 (Figure 3B) staining; recognizing that these changes represent trends across the cohort, but not necessarily robust statistical differences. Overall, staining intensity for IFNγ remained relatively consistent from baseline through year 2 for each of the five major leukocyte populations analyzed. Tracking individual nodes within the CD4 T cell population reveals an increase in IFNγ staining intensity in a few specific cell populations at month 2 that return to baseline staining patterns at years 1 and 2 (Figure 3A). While the same early time points could not be evaluated in the CyTOF and flow cytometry studies, the increased IFNγ staining in a subset of CD4 T cells at month 2 is consistent with the increased proportion of Th1 (CD45RA-CXCR3+CCR6-) effector cells revealed by flow cytometry at month 6 (Figure 2B).

Given the pathogenic role Th1 cells are believed to play in MS (*32, 33*), co-expression of IL-2 and TNFα were also examined in IFNγ high- and low- expressing nodes within the CD8 T cell compartment over time. Before HDIT/HSCT treatment, the majority of the IFNγ high-expressing cell populations co-expressed IL-2 and TNFα, whereas, the majority of IFNγ low-expressing populations consisted of single positive or double negative cells for IL-2 and TNFα (Figure 3A, dot plots). The polyfunctional staining profile of the IFNγ high-expressing CD8 T cells remained relatively stable at all time points evaluated post-HDIT/HSCT. In contrast, the proportion of

cells co-expressing IL-2 and TNFα increased in the in IFNγ low-expressing CD8 T cells at month 2, and returned to baseline staining patterns at years 1 and 2. (Figure 3A, dot plots).

T cell activation was evaluated together with cytokine production by tracking expression of surface markers PD-1, CD57, CD38 and HLA-DR over time. Figure 3B shows increased staining intensity of PD-1 on multiple CD4 and CD8 T cell populations at month 2 that return to baseline levels at years 1 and 2 with the exception of a few populations in the CD4 T cell compartment (Figure 3B). Co-expression of PD-1, CD57, CD38, and HLA-DR was examined in polyfunctional IFNγ high- and IFNγ low-expressing CD8 T cells (same clusters examined in Figure 3A). Prior to HDIT/HSCT treatment at baseline, most cells in the polyfunctional IFNγ high-expressing node exhibited intermediate levels of CD57 and HLA-DR with very few cells staining positive for PD-1 or CD38 (Figure 3B [same clusters as examined in Figure 3A]).

At 2 months post-HSCT the majority of polyfunctional CD8 T cells expressed CD38, and an increased proportion expressed PD-1 (Figure 3B top density plots), which is in contrast to the stable cytokine expression of the Th1 cells (Figure 3A). The majority of IFNγ low-expressing CD8 T cell populations lacked expression of PD-1, CD57, CD38 and HLA-DR prior to treatment. Striking alterations in the activation profile of these populations was observed at month 2 with the majority expressing high levels of CD57, CD38 and HLA-DR (Figure 3B lower density plots). These changes in activation profiles returned to baseline at years 1 and 2 for both IFNγ high- and low-expressing CD8 T cells.

Absolute Numbers of Memory CD4 and CD8 T cells in Peripheral Blood Prior to HDIT/HSCT and 5 Year Clinical Outcome

The cell profiles prior to treatment, and the repopulation kinetics post HDIT/HSCT treatment were examined to determine whether there were any biomarkers that correlated with the impressive 5-year clinical outcome of this Phase II study. Of the 23 participants that received HSCT, 16 maintained event-free survival through year 5, and 7 did not. None of the immune cell reconstitution or expression patterns at any of time point post HDIT/HSCT analyzed by CyTOF mass cytometry or multi-parameter flow cytometry correlated with the 5-year clinical outcome. However, prior to HDIT/HSCT treatment, the group of 16 patients that remained healthy throughout the 5-year study had significantly higher numbers of central memory (CD45RA-CCR7+) and effector memory (CD45RA-CCR7-) CD4 and CD8 T cells in peripheral blood than the 7 participants that experienced an MS-related event (Figure 4 A-D). Numbers of naïve (CD45RA+CCR7+) and EMRA (CD45RA+CCR7-) CD4 and CD8 T cells were similar between the two groups prior to treatment (Figure 4 E-H).

DISCUSSION

Technological advances in mass cytometry and multi-parameter flow cytometric analysis have dramatically improved our ability to monitor immunological changes associated with therapeutic intervention and disease activity. In the HALT-MS study, we previously used 5-color flow cytometric analysis of fresh peripheral blood to assess the reconstitution of major CD4 and CD8 T cells and B cell populations at 2 and 3 years post-HSCT (*12, 13*). One of the goals of this follow-up study was to use state-of-the-art analytic tools to complete a more comprehensive survey of the reconstitution kinetics of discrete populations of circulating leukocytes in these patients. Here, we were able to monitor surface phenotypes and intracellular cytokine profiles

simultaneously in multiple subsets of T cells as they repopulated in the peripheral blood of participants using CyTOF mass cytometry analysis of viably frozen PBMC. For example, this powerful tool revealed dynamic changes in activation profiles (upregulation of CD38 and PD-1) of polyfunctional (IFNg+TNF+IL2+) CD8 T cell subsets early in the reconstitution process. To our knowledge, this is the first analysis, in any disease setting, to use CyTOF for extensive multi-parameter immunophenotyping of peripheral blood in patients treated with high dose immunosuppressive therapy followed by autologous stem cell transplant. This in-depth reconstitution analysis builds upon what we and others have seen using lower resolution methods (ref. 12, 13, 34, 35) in MS and other autoimmune diseases.

We observed that the majority of differences in circulating leukocytes from baseline (prior to depletion) occurred early in the reconstitution process at 2-6 months post-HDIT/HSCT. As expected, monocytes and NK cells were proportionally more abundant than CD4 T cell and B cell populations. This likely reflects slower kinetics of CD4 T cell and B cell reconstitution in the periphery as previously reported (*12, 13, 34*). Consistent with prior reports, reconstituting cells in circulating CD4 and CD8 T cell compartments reflected a bias towards memory phenotype cells with a skewed distribution favoring effector memory and late effector subtypes (*12, 13, 34, 35*). The altered balance of memory/naïve subtypes in total CD4 and CD8 T cell populations analyzed by CyTOF was recapitulated in circulating CD25+CD127-/lo CD4 Tregs analyzed by flow cytometry. Taken together, these findings suggest HDIT/HSCT intervention results in an early bias towards memory subtypes in conventional and regulatory T cell populations during the reconstitution process in peripheral blood.

One of the most striking findings was increased PD-1 on multiple subsets of circulating CD4 and CD8 T cells, which paralleled the bias towards effector memory and late effector phenotypes during early immune reconstitution. PD-1 is a co-inhibitory receptor that serves as a negative regulator of T cell function, proliferation, and survival (36). PD-1 is rapidly upregulated on T cells after acute activation to help limit the initial T cell response to robust stimulation (37). PD-1 signaling is essential for maintaining lymphocyte homeostasis by preventing immune-mediated damage and inducing T cell exhaustion to persistent antigens, as demonstrated in chronic viral infection and tumor models (38, 39). This mechanism is also thought to be important for establishing self-tolerance during homeostatic proliferation in lymphopenic hosts (40). Therefore, we believe that the transient increase in PD-1 expressing T cells is likely the consequence of proliferation that occurs early after HDIT/HSCT in these lymphopenic MS patients. This observation is also consistent with a prior report of an independent cohort of MS patients treated with HSCT (41). Although this study is limited to the repopulation kinetics in MS patients post HDIT/HSCT, it is tempting to speculate that similar kinetics would be seen in other patients undergoing depletion-repopulation therapy.

Using multi-parameter flow cytometric analysis, we further characterized the reconstitution of different lineages of effector CD4 T cells in circulation post HDIT/HSCT and showed that the proportion of CXCR3+CCR6- Th1 effector memory cells was significantly increased, while the proportion of CXCR3+CCR6+ Th17.1 effector memory cells was decreased 6 months post-HSCT. This transient early bias towards a Th1 effector memory surface phenotype was paralleled by increased IFNγ staining intensity as revealed by CyTOF analysis in select subsets of CD4 T cells early after HDIT/HSCT, demonstrating a bias towards the Th1 phenotype in reconstituting

effector memory CD4 T cells. In contrast, IFNγ production in CD8 T cells remained relatively stable at all time points evaluated, with IFNγ high-expressing cells co-expressing other cytokines such as IL-2 and TNFα.

We were particularly interested in the kinetics of Th17.1 cell repopulation as these cells, along with Th1 cells, have been implicated in the pathogenesis of MS. Consistent with the hypothesis that depletion of these cells would be beneficial, these were one of the few subsets where decreases in proportion to total CD4 cells were sustained for the two years following transplant. Furthermore, MDR1 activity, which is a marker for a particularly pathogenic cell subset, decreased following transplant and the decrease was maintained over the course of the study. While this decrease in MDR1 activity was also observed for other effector T cell subsets, Th17.1 cells were the only subset where the decrease in MDR1 activity was sustained out to year 2. In all other subsets examined, MDR1 activity returned to baseline by year 2. Although this decrease in MDR1 activity in Th17.1 cells would be consistent with a positive clinical outcome, we observed this change in activity in all patients regardless of their disease status. In general, the repopulation of immune cell subsets progressed similarly out to 2 years for all patients studied regardless of clinical outcome. The inability to detect repopulation differences corresponding with disease outcome could be a function of examining the heterogeneous population of T cells rather than the minor population of MS antigen-specific cells, or it may be related to the limited sample size (n=16-23 total study subjects; 4/16-7/23 that did not maintain event-free survival) and/or heterogeneity in the clinical course (type of MS-associated event and/or time post-transplant event occurred) of the participants that did not achieve

treatment success out to year 5 years post-HSCT. Although none of the observed treatment effects correlated with clinical success, patients that remained healthy throughout the 5-year study had significantly higher absolute numbers of memory CD4 and CD8 T cells in the periphery prior to HDIT/HSCT treatment. This unexpected finding could indicate that subjects that respond well to HDIT/HSCT intervention have worse disease prior to treatment. Conversely, one could speculate that patients that do not respond favorably to HDIT/HSCT, have fewer numbers of effector and central memory T cells in peripheral blood prior to treatment because these potentially pathogenic T cells are instead infiltrating the CNS perpetuating the disease. It is also possible that this is a spurious finding unrelated to the T cell immunopathology in the CNS (*42*). Further investigation is warranted before drawing conclusions about T cell biomarkers that might be predictive of treatment success.

ACKNOWLEDGEMENTS

We are indebted to Gerald Nepom and Philip Bernstein for their valuable critiques and additions to this paper. This research was performed as a project of the Immune Tolerance Network, an international clinical research consortium headquartered at the Benaroya Research Institute and supported by the National Institute of Allergy and Infectious Diseases of

the National Institutes of Health under Award Number UM1AI109565. The content is solely the responsibility of the authors and does not necessarily represent the official views of the National Institutes of Health.

DISCLOSURES

The authors have no conflicts of interest to disclose.

REFERENCES

1. T. Chitnis, The role of CD4 T cells in the pathogenesis of multiple sclerosis. *Int Rev Neurobiol* **79**, 43-72 (2007).
2. J. M. Fletcher, S. J. Lalor, C. M. Sweeney, N. Tubridy, K. H. Mills, T cells in multiple sclerosis and experimental autoimmune encephalomyelitis. *Clin Exp Immunol* **162**, 1-11 (2010).
3. J. H. Anolik *et al.*, Delayed memory B cell recovery in peripheral blood and lymphoid tissue in systemic lupus erythematosus after B cell depletion therapy. *Arthritis Rheum* **56**, 3044-3056 (2007).
4. C. Chanvillard, R. F. Jacolik, C. Infante-Duarte, R. C. Nayak, The role of natural killer cells in multiple sclerosis and their therapeutic implications. *Front Immunol* **4**, 63 (2013).
5. N. Claes, J. Fraussen, P. Stinissen, R. Hupperts, V. Somers, B Cells Are Multifunctional Players in Multiple Sclerosis Pathogenesis: Insights from Therapeutic Interventions. *Front Immunol* **6**, 642 (2015).
6. A. P. Jones *et al.*, Circulating immune cells in multiple sclerosis. *Clin Exp Immunol*, (2016).

7. A. Bhattacharyya *et al.*, Autologous hematopoietic stem cell transplant for systemic sclerosis improves anemia from gastric antral vascular ectasia. *J Rheumatol* **42**, 554-555 (2015).
8. R. A. Nash *et al.*, High-dose immunosuppressive therapy and autologous hematopoietic cell transplantation for severe systemic sclerosis: long-term follow-up of the US multicenter pilot study. *Blood* **110**, 1388-1396 (2007).
9. M. C. Vonk *et al.*, Long-term follow-up results after autologous haematopoietic stem cell transplantation for severe systemic sclerosis. *Ann Rheum Dis* **67**, 98-104 (2008).
10. H. L. Atkins *et al.*, Immunoablation and autologous haemopoietic stem-cell transplantation for aggressive multiple sclerosis: a multicentre single-group phase 2 trial. *Lancet* **388**, 576-585 (2016).
11. G. J. H. M. Richard A. Nash MD, Michael K. Racke MD, Uday Popat MD, Steven M. Devine MD, Kaitlyn C. Steinmiller, MS, Linda M. Griffith MD, MHS, PhD Paolo A. Muraro MD,PhD, Harry Openshaw, MD, Peter H. Sayre MD, Olaf Stuve MD, Douglas L. Arnold MD, Mark H. Wener MD, George E. Georges, MD, Annette Wundes MD, George H. Kraft MD,MS and James D. Bowen MD High-Dose Immunosuppressive Therapy and Autologous HCT for Relapsing-Remitting MS (HALT-MS). *Neurology* (in press).
12. P. A. Muraro *et al.*, T cell repertoire following autologous stem cell transplantation for multiple sclerosis. *J Clin Invest* **124**, 1168-1172 (2014).
13. R. A. Nash *et al.*, High-dose immunosuppressive therapy and autologous hematopoietic cell transplantation for relapsing-remitting multiple sclerosis (HALT-MS): a 3-year interim report. *JAMA Neurol* **72**, 159-169 (2015).
14. M. L. Disis *et al.*, Maximizing the retention of antigen specific lymphocyte function after cryopreservation. *J Immunol Methods* **308**, 13-18 (2006).

15. D. Lin, S. Gupta, and H. T. Maecker, Intracellular Cytokine Staining on PBMCs Using CyTOFTM Mass Cytometry. *bio-protocol.org* **5: e1370**, (2015).

16. P. Qiu *et al.*, Extracting a cellular hierarchy from high-dimensional cytometry data with SPADE. *Nat Biotechnol* **29**, 886-U181 (2011).

17. V. Brucklacher-Waldert, K. Stuerner, M. Kolster, J. Wolthausen, E. Tolosa, Phenotypical and functional characterization of T helper 17 cells in multiple sclerosis. *Brain* **132**, 3329-3341 (2009).

18. C. J. Hedegaard *et al.*, T helper cell type 1 (Th1), Th2 and Th17 responses to myelin basic protein and disease activity in multiple sclerosis. *Immunology* **125**, 161-169 (2008).

19. F. Jadidi-Niaragh, A. Mirshafiey, Th17 cell, the new player of neuroinflammatory process in multiple sclerosis. *Scand J Immunol* **74**, 1-13 (2011).

20. J. S. Tzartos *et al.*, Interleukin-17 production in central nervous system-infiltrating T cells and glial cells is associated with active disease in multiple sclerosis. *Am J Pathol* **172**, 146-155 (2008).

21. U. Feger *et al.*, Increased frequency of CD4+ CD25+ regulatory T cells in the cerebrospinal fluid but not in the blood of multiple sclerosis patients. *Clin Exp Immunol* **147**, 412-418 (2007).

22. J. Haas *et al.*, Prevalence of newly generated naive regulatory T cells (Treg) is critical for Treg suppressive function and determines Treg dysfunction in multiple sclerosis. *J Immunol* **179**, 1322-1330 (2007).

23. J. Haas *et al.*, Reduced suppressive effect of CD4+CD25high regulatory T cells on the T cell immune response against myelin oligodendrocyte glycoprotein in patients with multiple sclerosis. *Eur J Immunol* **35**, 3343-3352 (2005).

24. H. Kebir *et al.*, Preferential recruitment of interferon-gamma-expressing TH17 cells in multiple sclerosis. *Ann Neurol* **66**, 390-402 (2009).

25. M. Kumar *et al.*, CD4+CD25+FoxP3+ T lymphocytes fail to suppress myelin basic protein-induced proliferation in patients with multiple sclerosis. *J Neuroimmunol* **180**, 178-184 (2006).

26. K. Venken *et al.*, Natural naive CD4+CD25+CD127low regulatory T cell (Treg) development and function are disturbed in multiple sclerosis patients: recovery of memory Treg homeostasis during disease progression. *J Immunol* **180**, 6411-6420 (2008).

27. K. Venken *et al.*, Secondary progressive in contrast to relapsing-remitting multiple sclerosis patients show a normal CD4+CD25+ regulatory T-cell function and FOXP3 expression. *J Neurosci Res* **83**, 1432-1446 (2006).

28. K. Venken *et al.*, Compromised CD4+ CD25(high) regulatory T-cell function in patients with relapsing-remitting multiple sclerosis is correlated with a reduced frequency of FOXP3-positive cells and reduced FOXP3 expression at the single-cell level. *Immunology* **123**, 79-89 (2008).

29. V. Viglietta, C. Baecher-Allan, H. L. Weiner, D. A. Hafler, Loss of functional suppression by CD4+CD25+ regulatory T cells in patients with multiple sclerosis. *J Exp Med* **199**, 971-979 (2004).

30. Y. D. Mahnke, T. M. Brodie, F. Sallusto, M. Roederer, E. Lugli, The who's who of T-cell differentiation: human memory T-cell subsets. *Eur J Immunol* **43**, 2797-2809 (2013).

31. R. Ramesh *et al.*, Pro-inflammatory human Th17 cells selectively express P-glycoprotein and are refractory to glucocorticoids. *J Exp Med* **211**, 89-104 (2014).

32. M. Sospedra, R. Martin, Immunology of multiple sclerosis. *Annu Rev Immunol* **23**, 683-747 (2005).

33. H. L. Weiner, Multiple sclerosis is an inflammatory T-cell-mediated autoimmune disease. *Arch Neurol* **61**, 1613-1615 (2004).

34. L. C. Arruda *et al.*, Immunological correlates of favorable long-term clinical outcome in multiple sclerosis patients after autologous hematopoietic stem cell transplantation. *Clin Immunol* **169**, 47-57 (2016).

35. M. Bosch, F. M. Khan, J. Storek, Immune reconstitution after hematopoietic cell transplantation. *Curr Opin Hematol* **19**, 324-335 (2012).

36. M. E. Keir, M. J. Butte, G. J. Freeman, A. H. Sharpe, PD-1 and its ligands in tolerance and immunity. *Annu Rev Immunol* **26**, 677-704 (2008).

37. G. J. Freeman *et al.*, Engagement of the PD-1 immunoinhibitory receptor by a novel B7 family member leads to negative regulation of lymphocyte activation. *J Exp Med* **192**, 1027-1034 (2000).

38. D. L. Barber *et al.*, Restoring function in exhausted CD8 T cells during chronic viral infection. *Nature* **439**, 682-687 (2006).

39. E. J. Wherry, M. Kurachi, Molecular and cellular insights into T cell exhaustion. *Nat Rev Immunol* **15**, 486-499 (2015).

40. S. J. Lin, C. D. Peacock, K. Bahl, R. M. Welsh, Programmed death-1 (PD-1) defines a transient and dysfunctional oligoclonal T cell population in acute homeostatic proliferation. *J Exp Med* **204**, 2321-2333 (2007).

41. L. C. Arruda *et al.*, Autologous hematopoietic SCT normalizes miR-16, -155 and -142-3p expression in multiple sclerosis patients. *Bone Marrow Transplant* **50**, 380-389 (2015).

42. S. Han *et al.*, Comprehensive immunophenotyping of cerebrospinal fluid cells in patients with neuroimmunological diseases. *J Immunol* **192**, 2551-2563 (2014).

Figure 1

Time course of immune cell reconstitution post-stem cell transplant for all HALT-MS patients, using concatenated data, visualized by SPADE trees constructed from a concatenated FCS file containing equal numbers of cell events from each patient for each time point. Major immune cell populations were grouped according to the SPADE analysis. Each node in the SPADE tree represents a cluster of cells that share a similar phenotype. Nodes in this SPADE tree are colored according to CD8 staining intensity and their size reflects number of cells within the cluster represented by that node. Pie charts are based on absolute cell numbers to illustrate the proportion of cell subsets within the major immune cell population. Absolute counts were calculated from SPADE analysis together with total lymphocyte counts from CBC. All cell subsets, except for $CD4^+$ T cells, were fully recovered by 2 years post-transplant. At 2 months, monocytes and NK cells are proportionally more abundant. There is also a redistribution of CD8+ T cell phenotypes, with a bias towards late effector phenotypes. At 1 and 2 years post-transplant, B cells are proportionally more abundant, and other populations more closely reflect baseline distributions. Naïve T cells: CD45RA+CCR7+; CM T cells: CD45RA-CCR7+; EM T cells: CD45RA-CCR7-; Effector T cells: CD45RA+CCR7-; Naïve B cells: IgD+CD27-; Memory B cells: IgD-CD27+CD38-; PC: IgD-CD27+CD38+

Figure 2

Changes in frequency of regulatory and effector CD4 T cells post-stem cell transplant. Flow cytometry was used to determine the frequency of A) regulatory T cells (Tregs: CD4+CD25+CD127-) and B) effector T cells (CD4+CD45RA- non-Tregs) as well as C) MDR1 activity of effector T cells using rhodamine efflux as a marker. For Tregs, the pie charts

represent the proportion of CD45RA+/- cells. For CD4+CD45RA- effector T cells, the line graphs in B) represent proportion of effector T helper cell lineage subsets and in C) represent the percent of cells in each effector subset that efflux rhodamine. A mixed model for repeated measurements was used to determine significant differences between time points for the mean of evaluated T cell subsets indicated by p values under the pie charts and on the line graphs (*p<0.01, **p<0.001).

Figure 3

Time course of cytokine production and PD1 expression during immune cell reconstitution post-stem cell transplant, visualized by SPADE. A) Nodes in this SPADE tree are colored according to IFNg staining intensity and their size reflects number of cells within the cluster represented by that node. Representative IFNg high- and low- expressing nodes in the CD8 T cell population were selected for further evaluation. Co-expression of IL-2 and TNF within these nodes were tracked over time (pop-out density plots). B) Nodes in this SPADE tree are colored by PD1 staining intensity and their size reflects number of cells within the cluster represented by that node. The same IFNg high- and low- expressing nodes selected in panel A were tracked over time for co-expression of PD1, CD57, HLA-DR and CD38 in panel B.

Figure 4

Absolute cell numbers for immune cell subsets grouped by the 5-year clinical outcome, which is defined as maintenance of event-free survival 5 years post-stem cell transplant. A) CM T cells: CD45RA-CCR7+; B) EM T cells: CD45RA-CCR7-; C) Naïve T cells: CD45RA+CCR7+; D) EMRA T cells: CD45RA+CCR7. Absolute counts were calculated from SPADE analysis together with total lymphocyte counts from CBC. Data shown are individual dot plots and group means +/- SEM for

the 15 participants that maintained event-free survival through year 5, and the 7 participants that did not. A mixed model for repeated measurements was used to determine significant difference between patient groups (**p<0.001, ***p<0.0001).

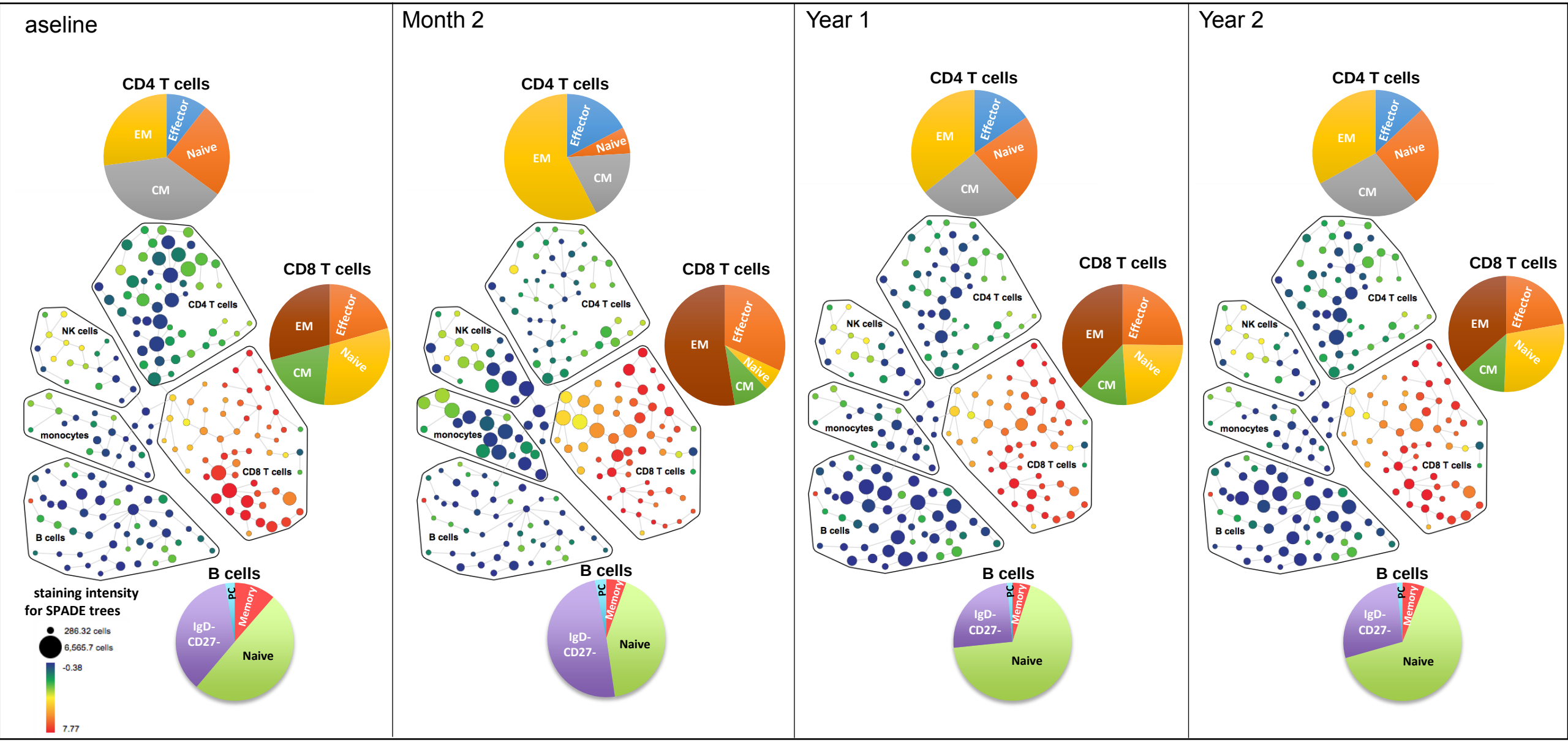

Figure 1

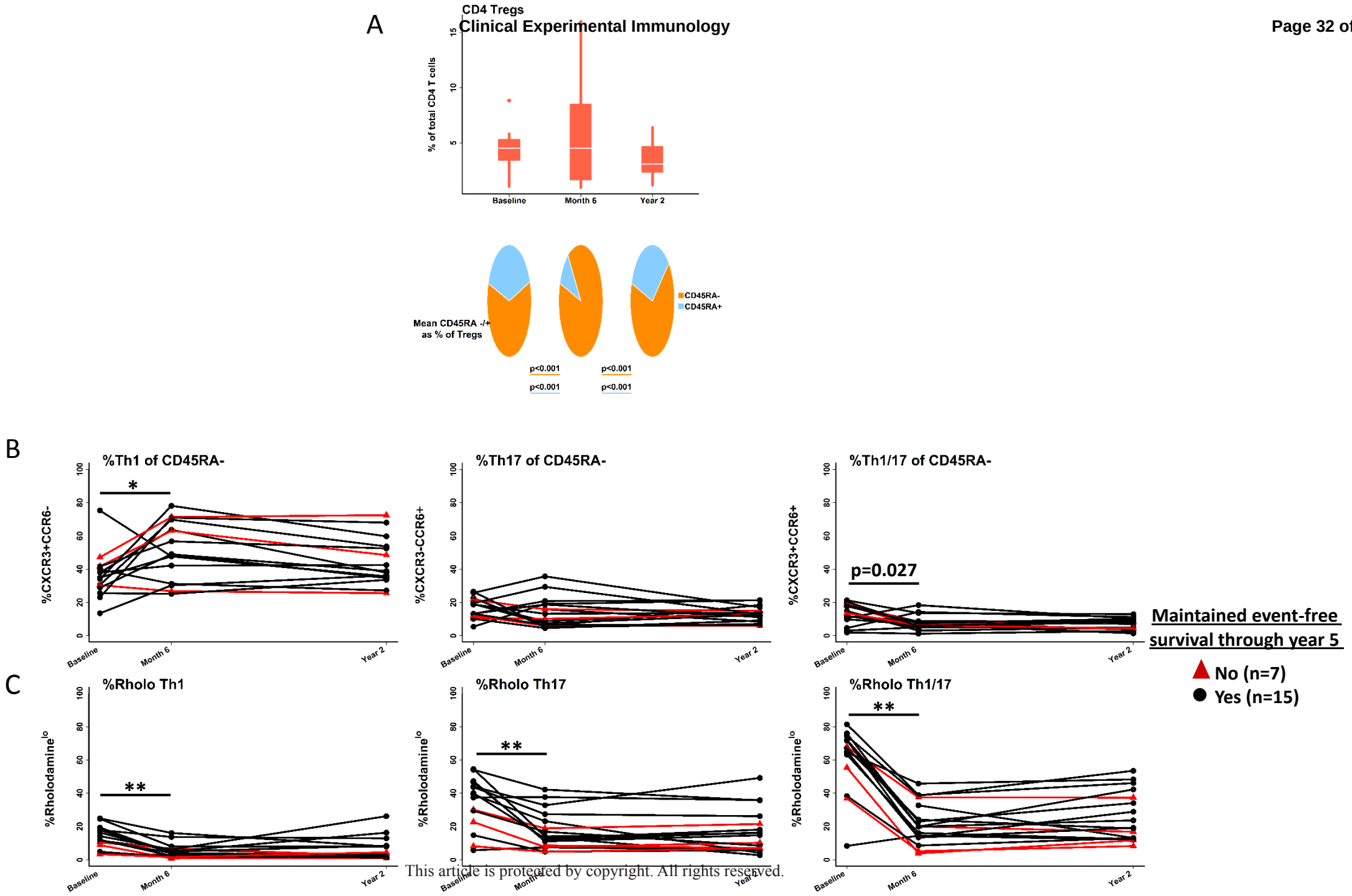

Figure 2

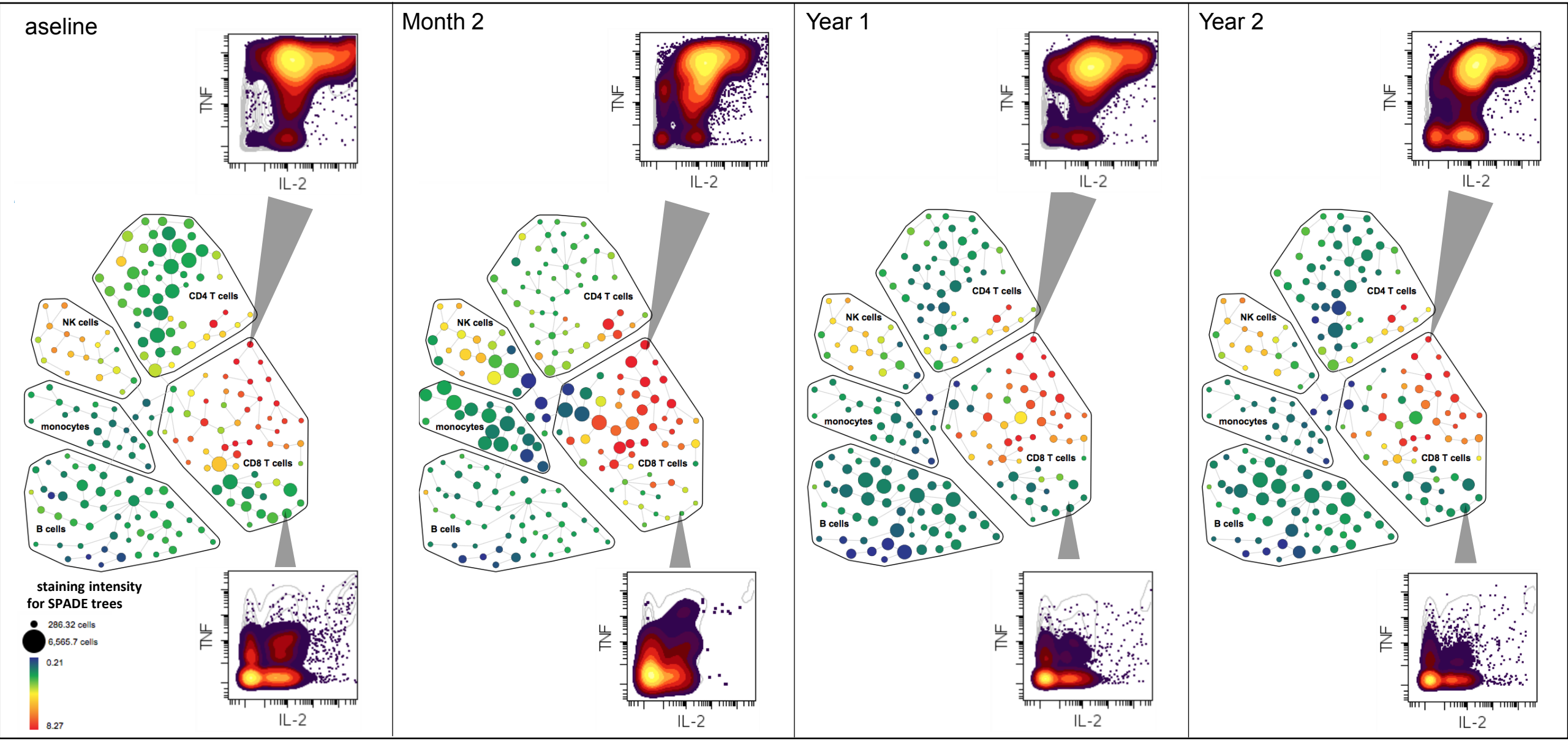

Figure 3A

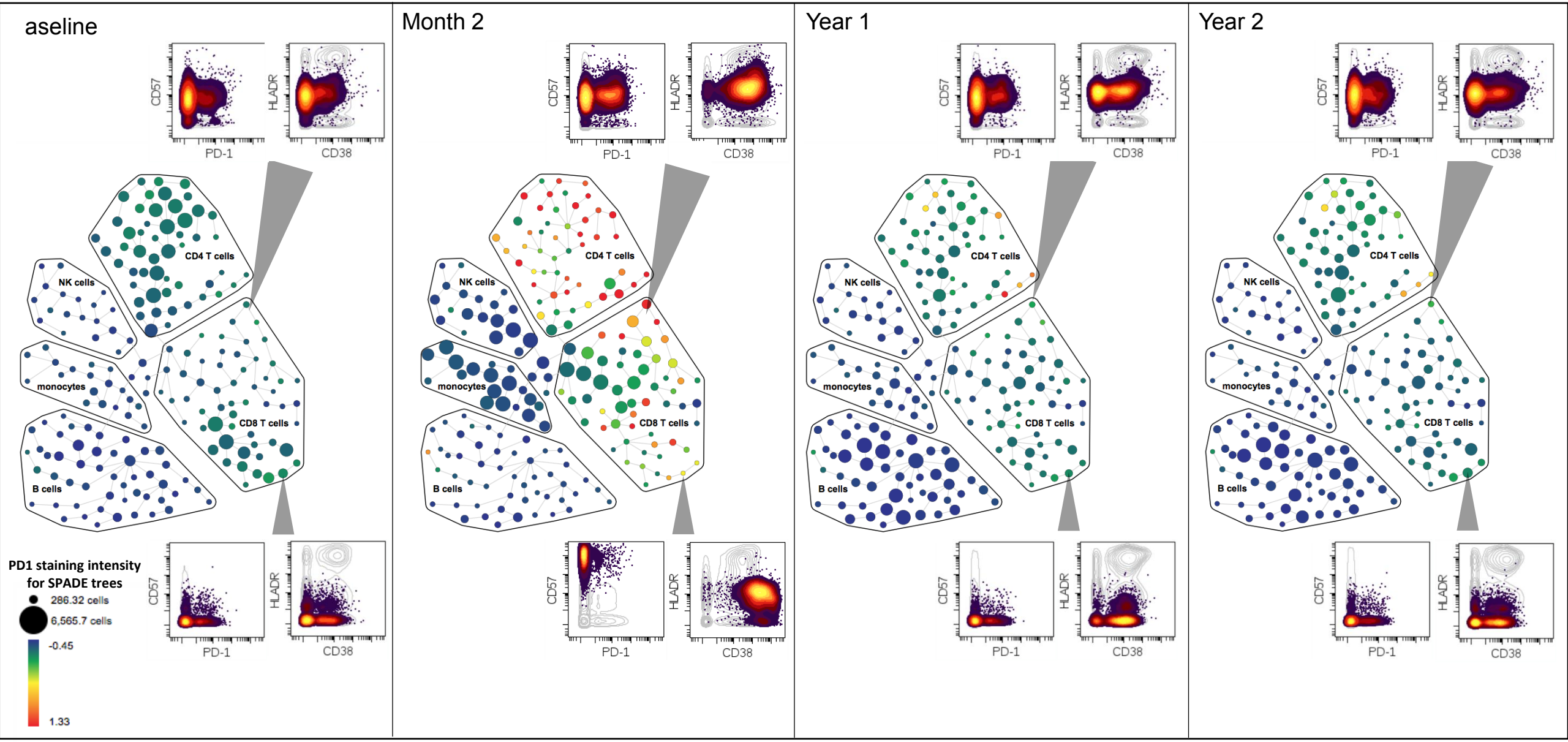

Figure 3B

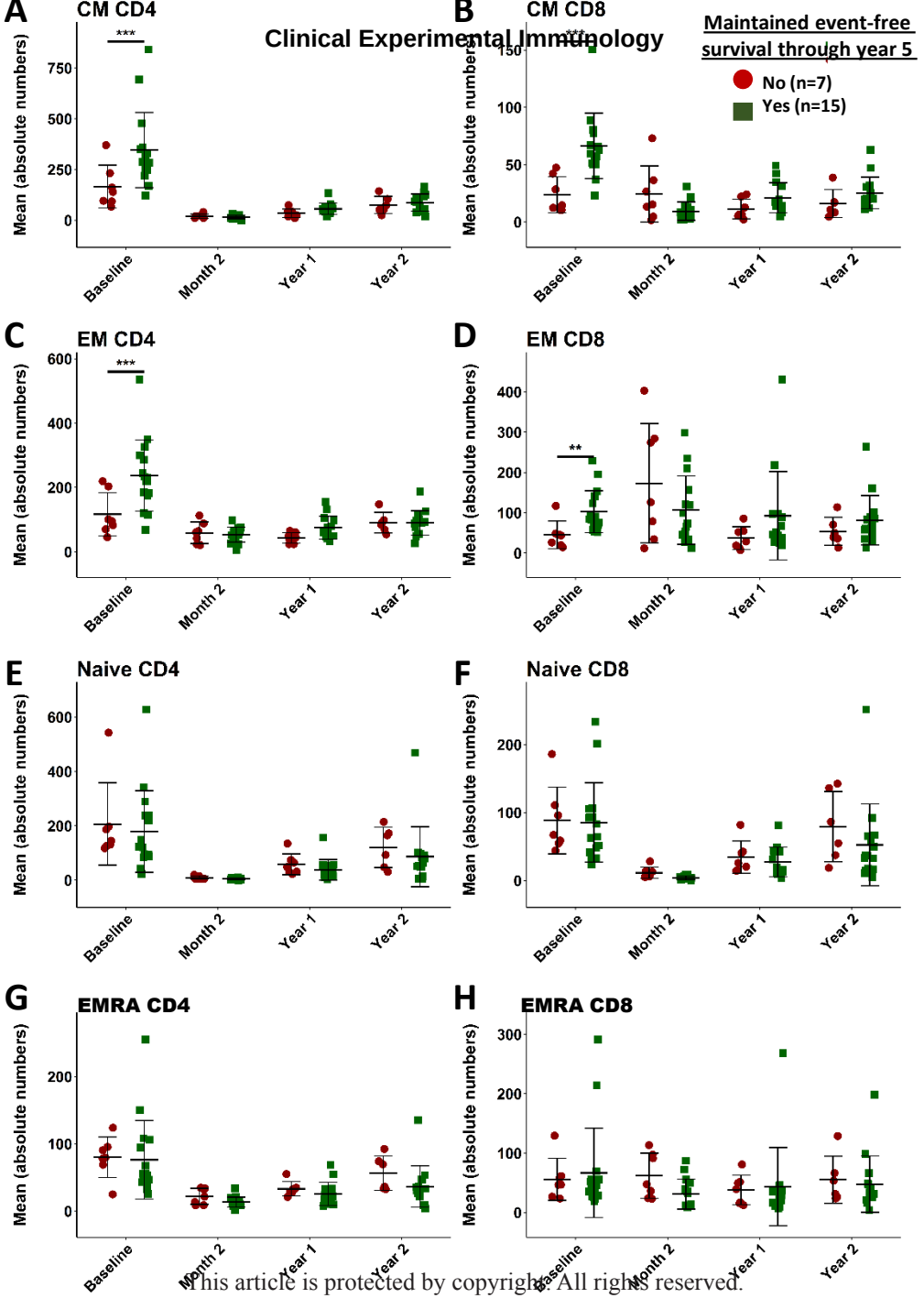

Figure 4